Thermochimica Acta, 105 (1986) 161–177
Elsevier Science Publishers B.V., Amsterdam – Printed in The Netherlands

SPECTROSCOPIC AND THERMAL CHARACTERIZATION OF SOME 5-ACETYL-4-β-D-GLYCOPYRANOSYLAMINOPYRIMIDINE DERIVATIVES AND THEIR ACETYLATED SUGAR HOMOLOGUES

R. LOPEZ GARZON *, A. SANCHEZ RODRIGO, M. NOGUERAS MONTIEL and J. NEGRILLO PEREZ

Departments of General and Organic Chemistry, University College, 23071 Jaén (Spain)

A.M. BERNALTE GARCIA

Department of Inorganic Chemistry, University of Extremadura, Badajoz (Spain)

(Received 4 February 1986)

ABSTRACT

Six 5-acetyl-4-β-D-glycopyranosylaminopyrimidine derivatives and their acetylated sugar homologues have been characterized by elemental analysis, IR and ^{1}H-NMR spectroscopy. Thermal study of the compounds shows four types of process: (i) desolvation; (ii) solid–solid transition; (iii) melting; (iv) pyrolytic decomposition. Probable mechanisms for the onset of pyrolytic decomposition are proposed.

INTRODUCTION

Pyrimidine derivatives, their nucleosides and some of their metal complexes are active in many biological processes [1,2] and the synthesis and characterization of these compounds are of increasing interest. In this paper we report the spectral and thermal characterization of the following two series of pyrimidine derivatives.

Apart from the essential interest of these compounds as potential antitumor agents, they may also be considered as possible ligands for transition metal ions. The data presented herein should be useful in assessing this property.

---

* To whom correspondence should be addressed.

0040-6031/86/$03.50

Compound	X	R	R_1	n
1A	O	H	CH_2OH	
1B	O	CH_3	H	1
1C	O	CH_3	CH_2OH	
1D	S	H	CH_2OH	
1E	S	CH_3	H	1/2
1F	S	CH_3	CH_2OH	1

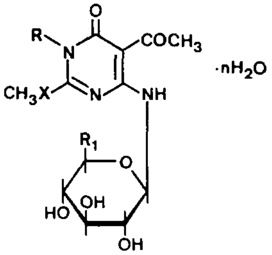

Compound	X	R	R_2
2A	O	H	CH_2OAc
2B	O	CH_3	H
2C	O	CH_3	CH_2OAc
2D	S	H	CH_2OAc
2E	S	CH_3	H
2F	S	CH_3	CH_2OAc

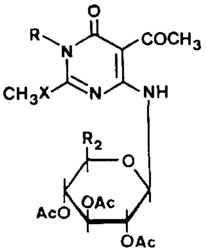

EXPERIMENTAL

All the compounds were obtained by reported methods [3]. Microanalyses were carried out at the Departament of Inorganic Chemistry, University of Extremadura, Badajoz. The analytical and yield data obtained, together with the corresponding formulae, are listed in Tables 1 and 2.

TABLE 1

Analytical and yield data of compounds of series 1

Compound	%C	%H	%N	Formula	Yield (%)
1A	45.73 (45.22)	5.69 (5.55)	11.72 (12.17)	$C_{13}H_{19}N_3O_8$	74
1B	45.25 (44.96)	5.66 (6.09)	11.81 (12.10)	$C_{16}H_{19}N_3O_7 \cdot H_2O$	79
1C	46.50 (46.80)	5.97 (5.89)	11.27 (11.69)	$C_{14}H_{21}N_3O_8$	91
1D	42.88 (43.21)	5.32 (5.30)	11.28 (11.63)	$C_{13}H_{19}N_3O_7S$	89
1E	44.92 (44.06)	5.93 (5.69)	12.38 (11.86)	$C_{13}H_{19}N_3O_6S \cdot 1/2H_2O$	98
1F	43.12 (42.74)	5.86 (5.89)	10.66 (10.68)	$C_{14}H_{21}N_3O_7S \cdot H_2O$	77

The analytical data in parentheses are theoretical values.

TABLE 2

Analytical and yield data of compounds of series 2

Compound	%C	%H	%N	Formula	Yield (%)
2A	48.91 (49.12)	5.34 (5.30)	8.02 (8.18)	$C_{21}H_{27}N_3O_{12}$	32
2B	50.41 (50.11)	5.75 (5.53)	9.12 (9.23)	$C_{19}H_{25}N_3O_{10}$	24
2C	50.33 (50.09)	5.65 (5.54)	7.87 (7.97)	$C_{22}H_{29}N_3O_{12}$	60
2D	47.90 (47.63)	5.29 (5.14)	7.87 (7.94)	$C_{21}H_{27}N_3O_{11}S$	46
2E	48.54 (48.40)	5.50 (5.34)	8.65 (8.91)	$C_{19}H_{25}N_3O_9S$	57
2F	48.68 (48.61)	5.49 (5.38)	7.67 (7.73)	$C_{22}H_{29}N_3O_{11}S$	71

The analytical data in parentheses are theoretical values.

The IR spectra were recorded with a Beckman 4250 spectrophotometer in the range 4000–200 cm^{-1}, with the compounds in KBr pellet form. The ^1H-NMR were obtained with a Hitachi Perkin-Elmer R-600 spectrophotometer in the range 0–20 ppm, using DMSO-d_6 and Cl_3CD solutions of each compound and TMS as interal standard.

TG curves were obtained with a Mettler TG 50 thermobalance in a static pure air atmosphere at a heating rate of 10°C min^{-1}, with samples of 6.68–14.17 mg. DSC plots were obtained with a Mettler DSC 20 differential scanning calorimeter at a heating rate of 5°C min^{-1}, using samples of 0.949–1.348 mg.

RESULTS AND DISCUSSION

Spectral study

The IR spectra of the six compounds of series 1 (Table 3) show several bands between 3700 and 3000 cm^{-1}, which have been assigned to ν(N–H) and ν(O–H) stretching vibrations and correspond to the N_1–H amino

TABLE 3

IR spectral data of compounds of series 1

Compound	ν(N–H) ν(O–H)	ν(C–H)	ν(C=O) 5-acetyl group	ν(C=O) 6-oxo group	ν(C=C) ν(C=N)	ν(C–N)	ν(C–O) δ(O–H)	ν(C–S)	Other bands
1A	3510 m	2950 w	1685 s	1670 s	1625 s	1330 s	1090 m		995 m
	3370 s	2920 w			1575 s	1285 s	1035 m		960 m
	3300 s	2880 w					1015 m		890 w
	3040 m	2830 w							760 w
									740 w
									695 w
1B	3490 m	2950 w	1665 s	1615 s	1560 s,wi	1310 m	1085 m		975 m
	3380 m	2910 w				1290 m	1075 m		960 m
	3200 s	2840 w				1215 m	1040 m		940 m
									890 w
									730 w
									680 w
1C	3450 s	2920 w	1665 s	1630 s	1570 s,wi	1320 m	1075 s		980 w
	3360 m					1290 m	1040 s		960 w
	3270 m					1255 m	1020 m		940 w
	3200 m					1215 m			890 w

									730 w
									675 w
1D	3540 w	2930 w	1670 s	1610 s	1580 s	1315 m	1105 m	650 w	980 m
	3510 m	2910 w			1550 s	1295 m	1080 s		940 w
	3400 m					1270 m	1060 m		890 w
	3360 m					1230 m	1045 s		815 w
	3250 w					1200 m			750 w
	3140 w								725 w
1E	3520 w	2920 w	1670 s	1610 s	1570 s	1305 m	1060 s	630 w	980 w
	3480 w	2840 w			1530 s	1275 m	1025 m		960 m
	3360 m					1255 m			930 w
	3280 w								890 w
	3100 w								740 w
									665 w
1F	3440 s	2960 w	1660 s	1625 s	1570 s	1310 m	1105 s	615 w	985 w
	3360 s,wi	2920 w			1535 s	1290 m	1075 s		960 w
		2880 w				1270 m	1040 s		940 w
						1250 m			900 w
						1215 m			740 w
									700 w

ν in cm^{-1}: w, weak; m, medium; s, strong; wi, wide.

groups (in compounds 1A and 1D), the C_4–NH amino groups, the –OH groups of the sugar molecules and the water of hydration molecules (in 1B, 1E and 1F). The high wavenumber values of these bands can be related to the intramolecular interactions through hydrogen bridges [4].

The bands appearing in the ranges 1685–1660 cm^{-1} and 1670–1610 cm^{-1} have been assigned to ν(C=O) stretching vibrations of C_5–$COCH_3$ and C_6=O carbonyl groups, respectively. The wavenumber values of stretching vibrations of C_6=O carbonyl groups are lower than those in the corresponding homologous compounds glycopyranosylaminopyrimidine derivatives [5]; this suggests probable intermolecular hydrogen bridge interactions through the C_6=O group.

The bands assigned to ν(C–O) and δ(O–H) vibrations are mainly due to the –OH groups linked to the carbon atoms of the pyranose ring. These bands occur at a lower wavenumber than those assigned to ν(C–N) stretching vibrations. The bands originating from the skeletal pyranose ring, which should appear in the range 960–750 cm^{-1} [6], have not been assigned because of the complexity of the spectra in this range.

On considering the ^{1}H-NMR spectral data from the compounds of series 1 [3], it is interesting to note that the chemical shift values of the signal due to C_4–NH groups in these compounds (between 10.80 ppm in compound 1F and 11.10 ppm in 1A) are higher than those corresponding to the respective homologous glycopyranosylaminopyrimidine derivatives (which occur in the range 7.25–7.40 ppm) [7]. This is probably due to the hydrogen bridge linking the C_4–NH amino groups and the oxygen atom of the acetyl groups substituted on carbon five, which weakens the N–H bond. Likewise, the resonance values for the C_4–NH signals in some homologous glycopyranosylamino-5-nitrosopyrimidine derivatives occur in a similar range (12.25–12.60 ppm) due to the fact that in those compounds the 4-amino and 5-nitroso groups also interact by hydrogen bridge. Moreover, coordinating the 5-nitroso compounds to the metallic ions Pd(II) and Au(III) through the –NO groups breaks the hydrogen bridge and the corresponding C_4–NH signals in the corresponding ^{1}H-NMR spectra are shifted to higher field values ($\Delta\delta \simeq 3.5$ ppm) [8].

The signals corresponding to the N_1–H groups in the ^{1}H-NMR spectra of the compounds 1A and 1D have not been observed probably due to the relative high protic character of such hydrogen atoms, so that the corresponding signals are probably included in those from the DMSO-d_6 water. The study of the acid behaviour of 5-nitroso derivatives which are homologous with 1A and 1D shows that those nitrogen atoms are more basic than the nitrogen atoms of the amino groups.

From this ^{1}H-NMR data, it could be expected that the compounds with a hydrogen atom substituted on nitrogen have a medium intensity acidic character (similar to that of the homologous 5-nitroso derivatives) and those with a methyl group on nitrogen one have a weak acidic character.

The assignments of bands corresponding to the 5-acetyl-4-β-D-(O)-acetyl)glycopyranosylaminopyrimidine derivatives (series 2) are summarized in Table 4. Given that all the compounds are anhydrous, the bands appearing in the range 3200–3000 cm^{-1} have been assigned to ν(N–H) stretching vibrations. The most noticeable fact, on comparing these spectra to those of the corresponding deacetylated sugars already discussed, is the appearance of a new band at about 1750 cm^{-1}, which has been assigned to ν(C=O) stretching vibrations of the acetate groups of the sugar residue. Finally, all the compounds present a new strong band at about 1240 cm^{-1}, which can be assigned to ν(C–O) stretching vibrations of the acetate sugar groups.

Considering signals from the N_1–H (in the compounds 2A and 2D) and C_4–NH amino groups in the ^{1}H-NMR spectra of these compounds [3], the corresponding resonance values are similar to those of the series 1 homologues (compound 2A, $\delta_{N_1-H} = 12.20$ ppm; compound 2D, $\delta_{N_1-H} = 12.50$ ppm. The resonance values of the C_4–NH groups occur between 10.80 ppm in 2F and 11.10 ppm in 2A). Thus, in these compounds also there will exist hydrogen bridge interactions between the C_4–NH amino groups and the C=O of the acetyl groups substituted on carbon five. Furthermore, the resonance values for the signals under consideration are similar, suggesting similar acid strengths for both the acetylated and non-acetylated sugar compounds

Thermal study

The TG curves of the compounds of series 1 and 2 are given in Figs. 1 and 2, respectively, and the corresponding DSC plots are given in Figs. 3 and 4, respectively. From all these curves, the thermal data given in Tables 5 and 6 were obtained.

Compounds of series 1

The TG and DSC curves of the six compounds of this series allow us to identify four types of process: (i) desolvation; (ii) solid–solid transition; (iii) melting; (iv) pyrolytic decomposition.

(i) Desolvations Compound 1B and 1F have a water molecule of hydration. The temperature values for dehydration (Table 5) have been obtained from the corresponding endothermic peak (Fig. 3). The ΔH values are relatively high in both cases (46.3 kJ mol^{-1} for 1B and 58.5 kJ mol^{-1} for 1F), which suggests hydrogen bonds occur between HO_2 molecules and the compounds.

Compound 1E has half a water molecule of hydration per molecule of compound. The expected endothermic peak gives an energy of 60.4 kJ mol^{-1} per mole of water, which also suggests the presence of hydrogen bridges.

(ii) Solid–solid transitions The compound 1D shows a weak endothermic peak (3.0 kJ mol^{-1}) at 198°C, and compound 1F shows a weak exothermic effect at 217°C (−7.7 kJ mol^{-1}). The corresponding TG curves do not show

TABLE 4

IR spectral data of compounds of series 2

Compound	ν(N–H)	ν(C–H)	ν(C=O) Acetate groups	ν(C=O) 5-acetyl group	ν(C=O) 6-oxo group	ν(C=C) ν(C=N)	ν(C–N) ν(C–O) Acetate groups	ν(C–O)	ν(C–S)	Other bands
2A	3130 w 3060 w	2960 w 2930 w	1750 s	1665 s	1630 s,wi	1630 s,wi 1580 s	1320 s 1290 s 1250 s 1230 s	1040 s,wi		970 w 905 w 760 w 740 w 710 w 685 w
2B	3200 w 3060 w	2960 w 2940 w 2920 w	1760 s	1685 s	1625 s	1595 s 1520 s	1310 w 1290 m 1245 s 1215 s	1060 s 1040 m 1030 m		975 w 905 w 870 w 750 w 715 w 675 w
2C	3260 w 3100-3000 w	2950 w	1750 s,wi	1685 s	1625 s	1605 s 1560 s	1370 w 1290 m 1240 s 1215 s	1090 m 1070 m 1040 s		970 w 940 w 910 w 870 w 740 w 710 w 675 w

2D	3360 s	2930 w	1750 s	1655 s	1625 s	1560 s,wi	1310 w	1070 m	600 w	970 w
	3190 w						1250 s	1045 s,wi		905 w
							1225 s			880 w
										830 w
										745 w
2E	3180 w	2940 w	1750 s	1685 s	1625 s,wi	1575 s	1310 w	1065 s	605 w	985 w
	3080 w	2930 w				1545 s	1280 w	1035 s		930 w
							1250 s			905 w
							1230 s			875 w
										740 w
2F	3200 w	2950 w	1760 s,wi	1680 s	1625 s	1580 s	1310 w	1070 m	605 w	1105 w
	3080 w					1535 s	1245 s	1040 s		980 w
							1220 s			955 w
										910 w

ν in cm^{-1}: w, weak; m, medium; s, strong; wi, wide.

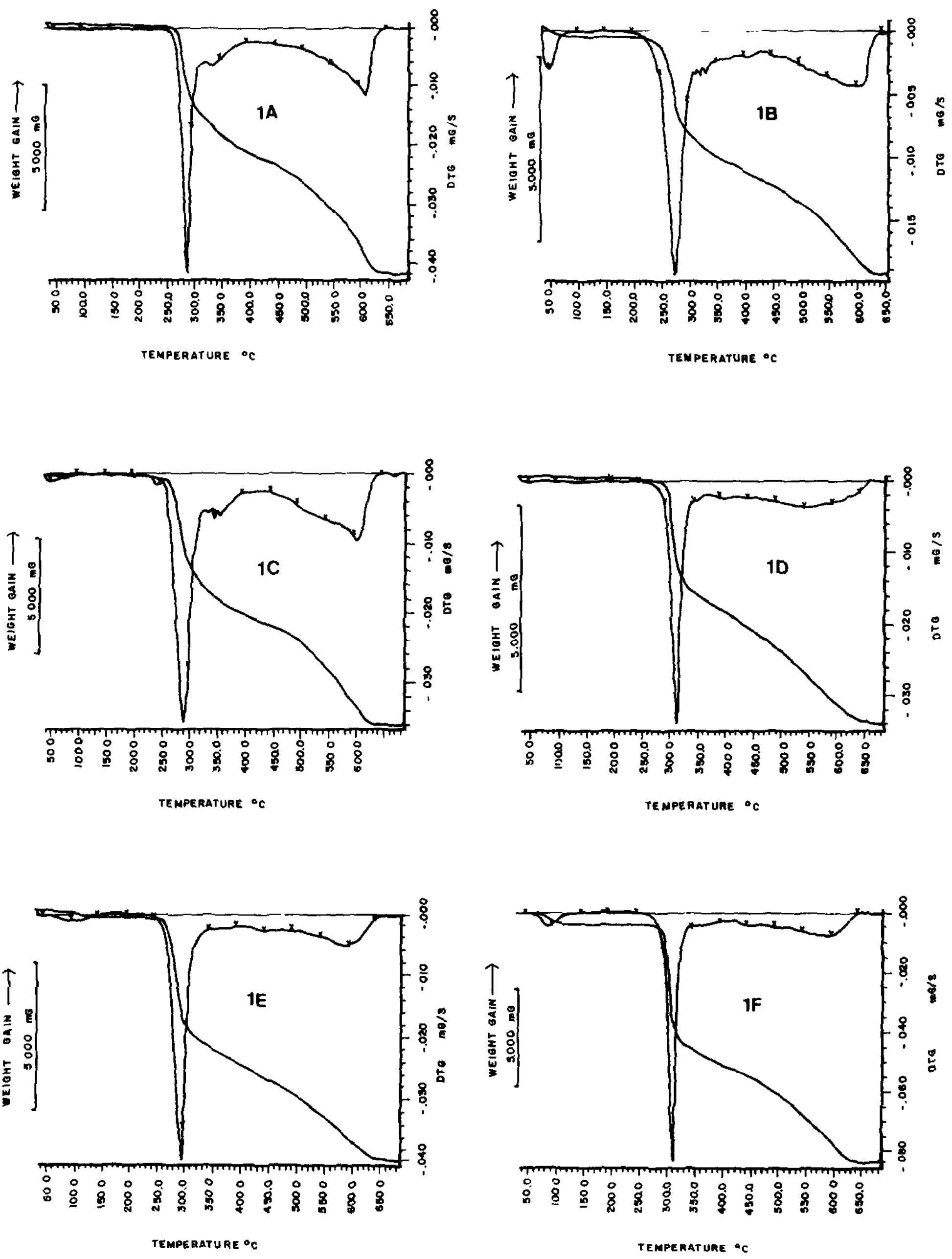

Fig. 1. TG curves of the compounds of series 1.

noticeable effects at these temperatures, and thus it is probable that they are caused by solid–solid changes of phase [9]. When a sample of each of the above compounds was heated up to the corresponding transition temperatures and their DSC plots were obtained after two hours, no noticeable

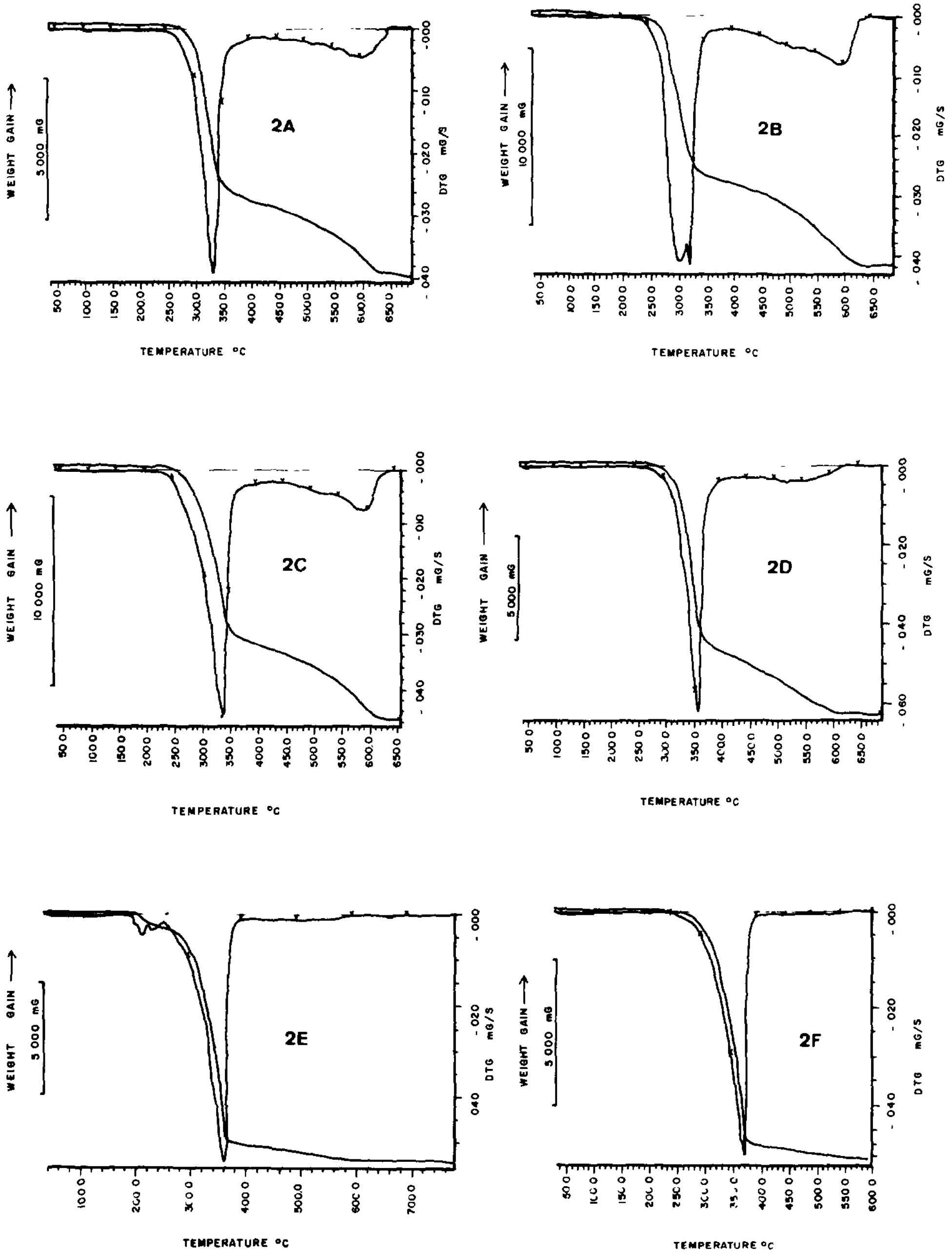

Fig. 2. TG curves of the compounds of series 2.

effects were observed at these temperatures. However the IR spectra of the heated samples were identical to those of the unheated samples.

All these data suggest that these effects correspond to some probably

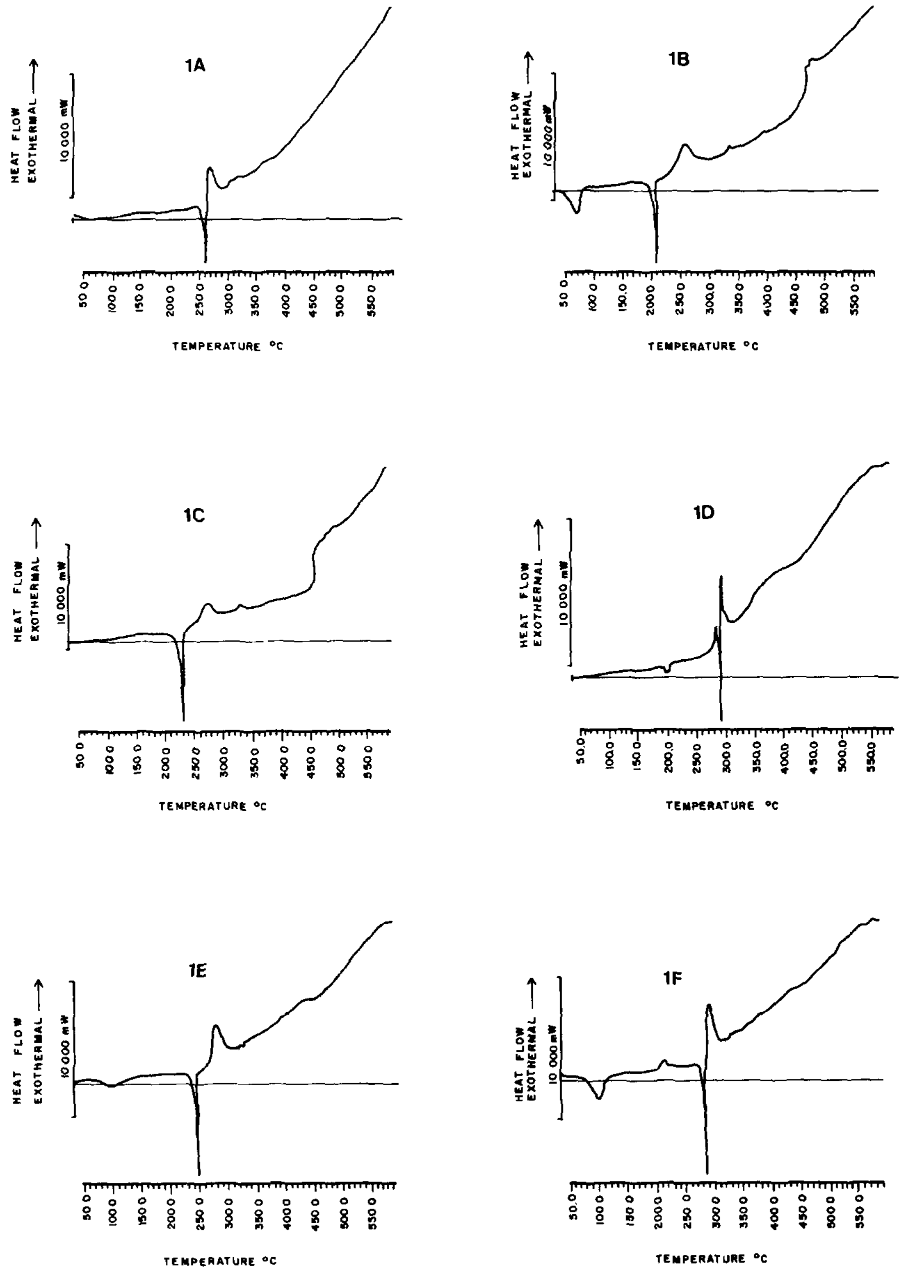

Fig. 3. DSC curves of the compounds of series 1.

irreversible solid–solid transitions, and do not imply any profound changes in the molecular structure of the compounds.

(iii) Melting All the compounds show melting processes before the start of their pyrolytic decomposition. The peak temperatures of the corresponding

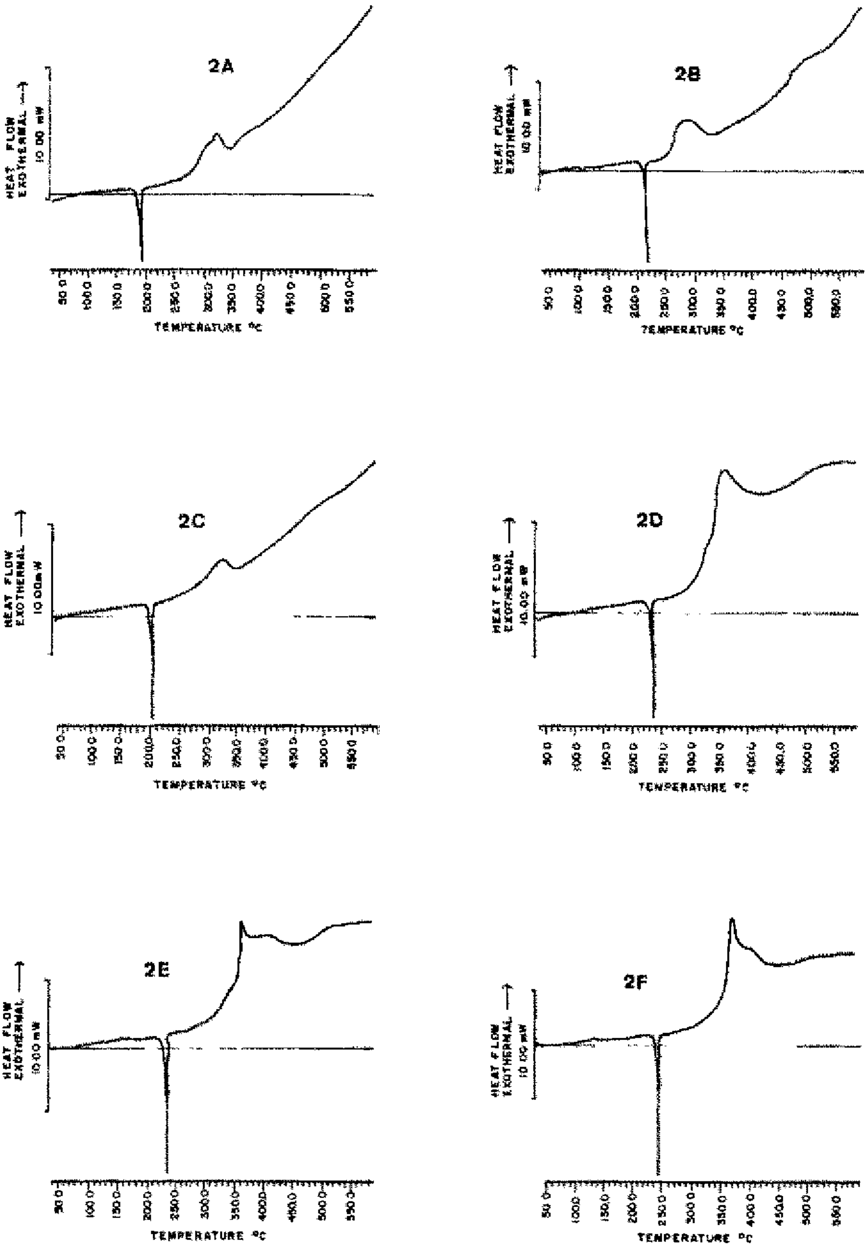

Fig. 4. DSC curves of the compounds of series 2.

endothermic effects (Fig. 3) are listed in Table 5. No weight losses occur in the TG plots over the temperature ranges in which the corresponding endothermic peaks occur.

The melting points do not increase in the same order as the molecular weights. This may be due to the importance of the hydrogen bridge inter-

TABLE 5

TG and DSC data of compounds of series 1

Compound	Desolvations			Solid–solid transitions		Melting		Start of pyrolysis		Other effects	
	T (°C)	Wt. loss (%)	ΔH (kJ mol^{-1})	T (°C)	ΔH (kJ mol^{-1})	T (°C)	ΔH (kJ mol^{-1})	T (°C)	ΔH (kJ mol^{-1})	T(°C)	ΔH (kJ mol^{-1})
1A						264 (258) [b]	29.0	273 exo [c]	−32.8	325 exo	–
1B	73	5.07 (5.18) [a]	46.3			209 (206) [b]	37.2	260 exo [c]	−89.3	337 exo	–
										473 exo	–
1C						231 (227) [b]	55.4	271 exo [c]	−59.2	331 exo	−8.9
										493 exo	–
1D				198 endo	3.0	292 (288) [b]	21.9	295 exo [c]	−19.6		
1E	101	2.78 (2.54) [a]	30.2			247 (236) [b]	39.4	281 exo [c]	−76.2	435 exo	−23.3
1F	102	4.65 (4.58) [a]	58.5	217 exo	−7.7	286 (275) [b]	43.3	298 exo [c]	−73.9	335 exo	–

[a] Theoretical values. [b] Melting temperature measured in a capillary. [c] Probable deacetylation and dehydroxylation.

TABLE 6

TG and DSC data of compounds of series 2

Compound	Melting		Start of pyrolysis		Other effects	
	T (°C)	ΔH (kJ mol^{-1})	T (°C)	ΔH (kJ mol^{-1})	T(°C)	ΔH (kJ mol^{-1})
2A	192 (187)	33.3	324 exo	−112.0		
2B	217 (212)	37.4	281 exo	−149.8		
2C	205 (202)	45.0	312 exo	−187.2		
2D	238 (231)	45.3	359 exo	−535.1		
2E	237 (231)	42.9	360 exo	−146.6	420 exo	−17.8
2F	242 (239)	54.9	377 exo	−643.2		

The melting temperatures in parentheses were measured in a capillary.

molecular interactions in the fusion processes. On comparing the melting points of compounds 1A, 1B and 1C (all with a methoxy substituent on carbon two) it can be seen that they increase in the same order as the number of potential hydrogen-bridging positions in the molecules (1B < 1C < 1A). At this point, only the hydroxyl groups on the sugar residues and on the nitrogen of the pyrimidine rings must be taken into account; the remaining potential hydrogen bridging positions (6-oxo, acetyl and amino groups) are present equally in all three compounds. The same is true of the melting points of compounds 1D, 1E and 1F, which are in the order 1E < 1F < 1D.

Finally, it is interesting to point out that the melting points of the compounds with methylthio groups on carbon two (1D, 1E and 1F) are higher than those of their homologues with methoxy substituents (e.g., $Pf_{1D} > Pf_{1A}$). This is due probably to the higher molecular weight of the methylthio derivatives.

(iv) Pyrolytic decomposition The temperatures corresponding to the onset of pyrolytic decomposition of all the compounds have been measured from the corresponding TG plots. For the compounds of series 1 these temperatures range between 220°C (compound 1C) and 280°C (compound 1D). The TG curves are quite alike in accordance with the similarity of their structures and this suggests analogous mechanisms for pyrolytic decomposition. In all the TG curves there appear three steps: the first is characterized by an abrupt weight loss, which ranges between 34.1% (compound 1A) and 41.2% (compound 1E); this step ends at temperature values between 270°C (compound 1B) and 320°C (compound 1D). The second step is characterized by a slow weight loss in the temperature range 300–390°C. Finally, abrupt weight losses between the last temperature and 650°C occur in all cases. At the final temperature there is no residue in the crucible.

The DSC plots of the six compounds of series 1 are also very similar. The abrupt weight losses corresponding to the first step in the TG plots are accompanied by an exothermic effect in the corresponding DSC. The six compounds under study were heated to the final temperature of this step and their IR spectra were recorded. In spite of the low resolution of these spectra (due probably to the carbon accumulated in the samples) the loss of the ν(C=O) and ν(C–O) stretching vibration bands of the acetyl groups and hydroxyl groups of the sugar residues respectively, is clear, while the other bands were practically unaffected. It was not possible to draw conclusions in the case of the weak ν(C–H) stretching vibration bands. The weight loss at the first TG step measured in the TG plots of the six compounds corresponds therefore to the loss of the acetyl groups, hydroxyl sugar groups and, if applicable the CH_2OH sugar group.

After the first exothermic effect, a second effect appears in all DSC plots (except that of compound 1D). Details are given in Table 5.

Compounds of series 2

The TG and DSC curves of the six compounds of this series are given in Figs. 2 and 4 respectively. All the compounds are anhydrous in accordance with the analytical data. The absence of water molecules could be due to the blocking of the oxygen atoms of the sugar residues by the acetate groups, resulting in a smaller number of hydrogen binding sites.

These compounds show two types of process: (i) melting; (ii) pyrolytic decompositions.

(i) Melting The six compounds of this series present a sharp endothermic effect at temperatures below their pyrolytic decomposition and no weight losses accompanying these effects appear in the corresponding TG plots. They were thus assigned to the corresponding melting processes. The temperature values for melting processes are generally lower (except for compound 2B) than those of the corresponding analogues of series 1; this is due to the blocking of the hydroxyl groups of the sugar residues, resulting in a diminition in the intensity of intermolecular interactions. On the other hand, compounds having methylthio groups as substituents on carbon two have higher melting points than their homologues with methoxy substituents, in accordance with the relative values of the molecular weights.

(ii) Pyrolytic decompositions The pyrolytic decomposition of all these compounds starts at about 250°C, similar to the series 1 compounds. All the processes occur in two steps, as can be seen in the corresponding TG plots. The first is characterized by an abrupt and considerable weight loss, which ends between 320°C (compound 2B) and 370°C (compound 2F). The second consists of a slow weight loss, which becomes complete at about 650°C with the total combustion of the samples.

The IR spectral study of samples from all the compounds, which were heated at increasing temperatures in the range corresponding to the first step of the pyrolytic decomposition, shows the progressive disappearance of the ν(C=O) stretching vibration bands assigned to acetyl groups together with those assigned to ν(C=O) and ν(C–O) of the sugar acetate groups. However, the progressive loss of resolution in the IR spectra of the heated samples, due to the accumulation of carbon in the samples, prevented establishment of the final temperature for these processes.

The DSC plots of the six compounds of this series show an exothermic effect approximately in the same temperature range as the first abrupt weight loss. The final temperatures of these exothermic effects are equal to those of the end of the first step in the TG plots in the cases of compounds 2A, 2B, 2C and 2D. However, the weight losses found in TG are slightly higher (about 5%) than those calculated for the theoretical whole deacetylation of the compounds.

In compounds 2E and 2F, the exothermic effects under study are asymmetrical, ending at higher temperature values than those corresponding to the end of the first step in the respective TG plots.

REFERENCES

1 R.M. Ottenbrite and G.B. Butler (Eds.), Anticancer and Interferon Agents, Vol. 24, Dekker, New York, 1984.

2 J.L. Rideout, D.W. Henry and M. Beacham (Eds.), Nucleosides, Nucleotides and their Biological Applications, Academic Press, New York, 1983.

3 J. Negrillo, M. Nogueras, A. Sànchez and M. Melgarejo, Monatsh. Chem., submitted.

4 L.J. Bellamy, The Infrared Spectra of Complex Molecules, 3rd edn., Chapman and Hall, London, 1975.

5 R. López Garzón, M. Nogueras Montiel, A. Sànchez Rodrigo, J. Negrillo Pérez and M. Bernalte García, Thermochim. Acta, 91 (1985) 173.

6 K. Nakanischi and P. Solomon, Infrared Absorption Spectroscopy, Holden-Day Inc., San Francisco, 1977.

7 M. Nogueras, Thesis, University of Granada, 1983

8 R. López Garzón, M.D. Gutiérrez Valero, A. Sànchez Rodrigo, M. Nogueras Montiel and C. Valenzuela Calahorro, Monatsh. Chem., in press.

9 M.I. Pope and M.D. Judd, Differential Thermal Analysis, Heyden, London, 1980.